

Tracking Control of Autonomous Underwater Vehicles with Internal Moving Mass

LI Jia-Wang¹ SONG Bao-Wei¹ SHAO Cheng¹

Abstract The trajectory-tracking control problem is investigated for an autonomous underwater vehicle (AUV) moving in the vertical plane using an internal point mass and a rear thruster as actuators. Combined with the dynamics of the point mass, the AUV is modeled as an underactuated system. A Lyapunov-based tracking controller is proposed by using backstepping approach to stabilize the error dynamics and force the position errors to a small neighborhood of the origin. Simulation results validate the proposed tracking approach.

Key words Autonomous underwater vehicle (AUV), moving mass, underactuated vehicle, tracking control

Traditional actuators of autonomous underwater vehicles (AUVs), such as fins and rudders, rely on relative fluid motion to provide control forces and torques, which will lose their control authority at very low speed. As an alternative means of control, moving mass control system (MMCS) may be invoked because it is entirely enclosed in the hull of vehicles and is equally effective in different conditions. Furthermore, MMCS can avoid corrosion and biological fouling. These advantages make MMCS very suitable for long-term ocean missions^[1].

During the past several years, many researchers have investigated the applicability of MMCS to space/underwater vehicles. Menon^[2] studied the integrated guidance and control problem of kinetic warheads actuated by three moving masses. The ability of an MMCS to control the attitudes of spinning vehicles and a fixed-trim reentry vehicle were investigated in [3–4], respectively. In underwater applications, the authors in [1, 5] studied the problem of stabilization for a neutrally buoyant underwater vehicle using internal rotors and a moving mass as actuators, respectively, and Leonard and Graver^[6] studied the controllability of buoyancy-propelled and fixed-wing underwater gliders using movable internal masses as attitude control actuators. However, except in [1, 5], the dynamics of the system or the control laws were linearized in these published works.

In this paper, we address the tracking control problem for AUVs using a rear thruster and an internal movable point mass as actuators without linearizing the system dynamics. For simplicity, we restrict our attention to vertical plane cases. In order to reduce the complexity of the integral controller designing course, we split it into two steps: we first calculate the desired value of the thrust force and the displacement of the point mass for the AUV by regarding the interacting forces as a part of model uncertainties, and then, we determine the control force actuating on the point mass because of the commanded displacement.

Furthermore, since the AUV has two independent control inputs less than degrees of freedom, the system that contains the AUV and the point mass is underactuated. For this system, tracking controller using nonlinear Lyapunov-based techniques is very suitable. Some examples of nonlinear Lyapunov-based trajectory-tracking controllers for un-

deractuated marine vehicles have been reported in [7–9]. Motivated by the results of [7], we develop a simple nonlinear control law for the tracking problem. Furthermore, we present a point mass positioning controller by means of a cascaded approach.

The rest of this paper is organized as follows: in Section 1, we describe the dynamic model for the AUV and the point mass. In Section 2, we present a nonlinear tracking control law and discuss the stability of the resulting closed-loop system. A point mass positioning controller is designed in Section 3. Section 4 illustrates the performance of the proposed method and some conclusions are given in Section 5.

1 AUV model

We model the vehicle as a rigid elliptical hull that encloses a movable point mass, as shown in Fig. 1. To describe the motion of the vehicle, we introduce two coordinate frames that will be used in the following sections. Oxy is an inertial reference frame (I-frame) fixed in space, and Bx_By_B is a body-fixed orthonormal frame (B-frame) with origin located at the center of buoyancy (CB) of the vehicle. Assume that the movable mass can move along the Bx_B -axis in a smooth slot.

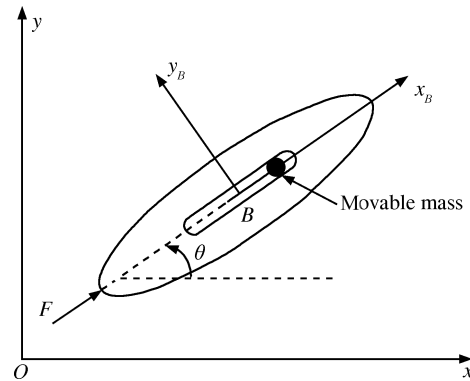


Fig. 1 The AUV and an internal movable mass

The total mass of the AUV, m_0 , contains two terms: m_h is the mass of the hull uniformly distributed throughout the ellipse, and m is the internal moving point mass. Let s denote the distance of the moving point mass that offsets from the CB, and $s \in [-l/2, l/2]$, where l is a positive scalar, denoting the length of the slot. We assume that $s|_{t=0}=0$, and thus, the center of mass (CM) of the AUV initially coincides with the CB.

Let $\mathbf{q} = [x, y]^T$ and θ be the position of the CB in the I-frame and the orientation of the vehicle, respectively. In the vertical plane, the kinematic equations of motion for the AUV can be written as

$$\begin{bmatrix} \dot{\mathbf{q}} \\ \dot{\theta} \end{bmatrix} = \begin{bmatrix} R(\theta) & 0 \\ 0 & 1 \end{bmatrix} \begin{bmatrix} \mathbf{v} \\ r \end{bmatrix} \quad (1)$$

where the upper dots represent differentiation with respect to time. $\mathbf{v} = [u, v]^T$ denotes a vector of the linear velocities in surge and heave, and r represents the angular velocity in pitch, decomposed in the B-frame. The matrix $R(\theta) \in \mathbf{R}^{2 \times 2}$ is a transformation matrix from the B-frame to the I-frame and can be written in a component form as

$$R(\theta) = \begin{bmatrix} \cos \theta & -\sin \theta \\ \sin \theta & \cos \theta \end{bmatrix}$$

Received August 3, 2007; in revised form December 24, 2007

1. College of Marine, Northwestern Polytechnical University, Xi'an 710072, P. R. China

DOI: 10.3724/SP.J.1004.2008.01319

Assume that: 1) the AUV is neutrally buoyant, i.e., $m_0 = m_h + m$ is equal to the mass of fluid displaced by the vehicle; 2) the inertia, added mass, and damping matrices are diagonal, and the drag terms of order higher than two can be neglected. The second assumption holds because the AUV introduced in this paper has two planes of symmetry, for which the axes of the B-frame coincide with the principal axes of the displaced fluid, and the vehicle moves slowly. In reality, most underwater vehicles have fore/aft non-symmetry, which implies that the off-diagonal terms of the inertia and damping matrices are nonzero. However, these terms are smaller than the diagonal terms. Therefore, the mathematic model of the vehicle moving in the vertical plane under environmental disturbances and model uncertainties can be expressed as in [10]

$$\begin{cases} m_{11}\dot{u} = m_{22}vr - X_uu - X_{u|u}|u| + F + w_1 + \tau_{d1} \\ m_{22}\dot{v} = -m_{11}ur - Y_vv - Y_{v|v}|v| + w_2 + \tau_{d2} \\ m_{33}\dot{r} = (m_{11} - m_{22})uv - N_r r - N_{r|r}|r| + w_3 + \tau_{d3} \end{cases} \quad (2)$$

where $m_{ii} (> 0)$ are the combination of the vehicle, added mass and inertia terms, and F denotes the thrust force along the longitudinal axis of the vehicle, X_u , $X_{u|u}$, Y_v , $Y_{v|v}$, N_r , and $N_{r|r}$ are the linear and quadratic damping terms coefficients, w_i represent the reacting forces and torque caused by the movement of the internal point mass and τ_{di} are bounded disturbances.

As depicted in Fig. 1, the kinetic equations of the internal point mass can be expressed in a compact form as

$$m[\dot{\boldsymbol{\nu}} + S(1)(\boldsymbol{\nu} + \boldsymbol{\xi} + S(1)\boldsymbol{\xi}r + 2\dot{\boldsymbol{\xi}})r + \ddot{\boldsymbol{\xi}}] = -\boldsymbol{\tau} + \mathbf{G}_m \quad (3)$$

where $\boldsymbol{\xi} = [s, 0]^T$ is a radius vector of the point mass in the B-frame, and $S(1)$ represents a skew-symmetric matrix and is given by $S(1) = \begin{bmatrix} 0 & -1 \\ 1 & 0 \end{bmatrix}$, $\boldsymbol{\tau}$ denotes a vector of the servo forces to actuate the vehicle on the point mass and $\mathbf{G}_m = [-mg \sin \theta, -mg \cos \theta]^T$ is a vector of the gravity of the point mass expressed in the B-frame.

Substituting (3) into (2) and rearranging, we can derive the accurate expressions about w_1 , w_2 , and w_3 as

$$\begin{cases} w_1 = -m(\ddot{s} - sr^2) \\ w_2 = -m(2\dot{s}r + s\dot{r}) \\ w_3 = s(-mg \cos \theta - m\dot{v} - mur + w_2) \end{cases} \quad (4)$$

In (2), there is a single explicit control force F , which makes it hard to design a control law for the AUV. Combining it with (4), we choose the variable s as another control parameter usable to produce a control torque. In order to express s explicitly, we can split the term w_3 into two parts: $w_3 = -sA + w'_3$, where $A = m(g \cos \theta + \dot{v} + ur)$ and $w'_3 = sw_2$ are the linear and nonlinear terms about s , respectively (In several conditions, the term $(g \cos \theta + \dot{v} + ur)$ may be equal to zero. To avoid this, we can regulate the expressions of A and w'_3 at real time in the course of calculation). Thus, we can rewrite (2) in a more concise form, for convenient in the following discussions, as

$$\begin{cases} M\dot{\boldsymbol{\nu}} = -S(1)M\boldsymbol{\nu}r - D(\boldsymbol{\nu})\boldsymbol{\nu} + \mathbf{g}_\nu F + \mathbf{w} \\ m_{33}\dot{r} = (m_{11} - m_{22})uv - N_r r - N_{r|r}|r| - sA + w''_3 \end{cases} \quad (5)$$

where $M = \text{diag}\{m_{11}, m_{22}\}$ is the generalized mass matrix, $D(\boldsymbol{\nu}) = \text{diag}\{X_u + X_{u|u}, Y_v + Y_{v|v}\}$, $\mathbf{g}_\nu = [1, 0]^T$, $\mathbf{w} = [w_1 + \tau_{d1}, w_2 + \tau_{d2}]^T$, and $w''_3 = w'_3 + \tau_{d3}$.

2 Controller design and analysis

In this section, we seek to design a trajectory-tracking control law for system (5) that forces it to track a given smooth geometric path in the vertical plane. In order to simplify the subsequent control development, we regard the terms w_1 , w_2 , and w'_3 as a part of model uncertainties to be determined in the next section.

Let $\mathbf{q}_d = [x_d, y_d]^T$ denote the desired position of the CB, where we define the following global invertible transformation

$$\mathbf{e}_q = R^T(\mathbf{q} - \mathbf{q}_d)$$

which expresses the tracking error $(\mathbf{q} - \mathbf{q}_d)$ in the B-frame. R^T is the transpose of the matrix $R(\theta)$ and its time derivative $\dot{R}^T = -S(1)R^T r$. The time derivative of \mathbf{e}_q becomes

$$\dot{\mathbf{e}}_q = -S(1)\mathbf{e}_{qr} + \boldsymbol{\nu} - R^T\dot{\mathbf{q}}_d \quad (6)$$

In the rest of this section, for the sake of clarity, we split our design procedure into two steps.

Step 1. (Design of the surge force F): We start by defining a Lyapunov function candidate as

$$V_1 = \frac{1}{2}\mathbf{e}_q^T \mathbf{e}_q$$

and computing its time derivative along the system trajectories to obtain

$$\dot{V}_1 = \mathbf{e}_q^T(\boldsymbol{\nu} - R^T\dot{\mathbf{q}}_d) \quad (7)$$

We can treat $\boldsymbol{\nu}$ as a virtual control to stabilize the tracking error \mathbf{e}_q . Unlike the standard compensating method, in order to reduce the complexity of the controller expressions, we will choose a simpler virtual control law $\boldsymbol{\nu}^d$ for $\boldsymbol{\nu}$ as

$$\boldsymbol{\nu}^d = -k_e M^{-1}\mathbf{e}_q$$

with $k_e > 0$ a design parameter to be determined later. Introducing the new error variable $\mathbf{z}_1 = \boldsymbol{\nu} - \boldsymbol{\nu}^d$ which we would derive to zero, (7) gives

$$\dot{V}_1 = -k_e \mathbf{e}_q^T M^{-1}\mathbf{e}_q + \mathbf{e}_q^T \mathbf{z}_1 - \mathbf{e}_q^T R^T \dot{\mathbf{q}}_d \quad (8)$$

By taking the time derivative of \mathbf{z}_1 and using (5), we get

$$M\dot{\mathbf{z}}_1 = -S(1)M\mathbf{z}_1 r + \mathbf{g}_\nu F + \mathbf{h}(\cdot) \quad (9)$$

where

$$\mathbf{h}(\cdot) = -D(\boldsymbol{\nu})\boldsymbol{\nu} + \mathbf{w} + k_e(\boldsymbol{\nu} - R^T\dot{\mathbf{q}}_d)$$

As introduced in [7], because of the coupling of the translation dynamics and the rotational inputs, the error \mathbf{z}_1 can not be ensured to converge to zero, yet it can be always forced to a small neighborhood of the origin. To this end, we define a new error variable $\mathbf{z}_2 = \mathbf{z}_1 - \boldsymbol{\delta}$ which we will derive to zero, and in which $\boldsymbol{\delta} \in \mathbf{R}^{2 \times 1}$ is a given constant vector. Substituting \mathbf{z}_2 into (8), we obtain

$$\dot{V}_1 = -k_e \mathbf{e}_q^T M^{-1}\mathbf{e}_q + \mathbf{e}_q^T \boldsymbol{\delta} - \mathbf{e}_q^T R^T \dot{\mathbf{q}}_d + \mathbf{e}_q^T \mathbf{z}_2$$

To stabilize the error vector \mathbf{z}_2 , we consider the following Lyapunov function candidate

$$V_2 = V_1 + \frac{1}{2}\mathbf{z}_2^T M^2 \mathbf{z}_2 = \frac{1}{2}\mathbf{e}_q^T \mathbf{e}_q + \frac{1}{2}\mathbf{z}_2^T M^2 \mathbf{z}_2$$

The time derivative of V_2 along the system trajectories can be expressed as

$$\begin{aligned} \dot{V}_2 = & -k_e \mathbf{e}_q^T M^{-1}\mathbf{e}_q + \mathbf{e}_q^T \boldsymbol{\delta} - \mathbf{e}_q^T R^T \dot{\mathbf{q}}_d + \\ & \mathbf{z}_2^T (M\mathbf{B}\boldsymbol{\sigma} + M\mathbf{h}(\cdot) + \mathbf{e}_q) \end{aligned} \quad (10)$$

where $B = [\mathbf{g}_\nu - S(1)M\boldsymbol{\delta}] \in \mathbf{R}^{2 \times 2}$, $\boldsymbol{\sigma} = [F, r]^T$ is regarded as a virtual control. Letting $\boldsymbol{\delta} = [\delta_1, \delta_2]^T$ be nonzero, and using (5), we can rewrite B in a component form as

$$B = \begin{bmatrix} 1 & m_{22}\delta_2 \\ 0 & -m_{11}\delta_1 \end{bmatrix}$$

One can see that the matrix B will be made full rank if and only if $\delta_1 \neq 0$. To stabilize the error variable \mathbf{z}_2 , we set $\boldsymbol{\sigma}$ at

$$\boldsymbol{\sigma} = B^{-1}(-\mathbf{h}(\cdot) - M^{-1}\mathbf{e}_q) - k_z M^{-1}\mathbf{z}_2$$

where k_z is a positive constant to be chosen later. Now, we set the surge force F at

$$F = [1, 0]\boldsymbol{\sigma} \quad (11)$$

Step 2. (Design of the displacement s): In the end of Step 1, we regard the angular velocity r as a part of the virtual control $\boldsymbol{\sigma}$. Since r is not a true control, we need to introduce a new error variable $z_3 = r - [0, 1]\boldsymbol{\sigma}$ which should be set at zero. Now, we can rewrite (10), with F given by (11), as

$$\begin{aligned} \dot{V}_2 = & -k_e \mathbf{e}_q^T M^{-1} \mathbf{e}_q + \mathbf{e}_q^T - \mathbf{e}_q^T R^T \dot{\mathbf{q}}_d - \\ & k_z \mathbf{z}_2^T \mathbf{z}_2 - \mathbf{z}_2^T M S(1) M \boldsymbol{\delta} z_3 \end{aligned} \quad (12)$$

Therefore, our objective in this step is to stabilize the error variable z_3 . Considering the following Lyapunov function candidate

$$V_3 = V_2 + \frac{1}{2} m_{33} z_3^2 = \frac{1}{2} \mathbf{e}_q^T \mathbf{e}_q + \frac{1}{2} \mathbf{z}_2^T M^2 \mathbf{z}_2 + \frac{1}{2} m_{33} z_3^2$$

and taking the time derivative, we obtain

$$\begin{aligned} \dot{V}_3 = & -k_e \mathbf{e}_q^T M^{-1} \mathbf{e}_q + \mathbf{e}_q^T \boldsymbol{\delta} - \mathbf{e}_q^T R^T \dot{\mathbf{q}}_d - k_z \mathbf{z}_2^T \mathbf{z}_2 + \\ & z_3 (h_1(\cdot) - sA - [0, m_{33}]\dot{\boldsymbol{\sigma}} - \mathbf{z}_2^T M S(1) M \boldsymbol{\delta}) \end{aligned} \quad (13)$$

where $h_1(\cdot) = (m_{11} - m_{22})uv - N_r r - N_{r|r}|r| + w''_3$, and $\dot{\boldsymbol{\sigma}}$ stands for the time derivative of $\boldsymbol{\sigma}$. If we then set s at

$$s = \frac{1}{A} (h_1(\cdot) - [0, m_{33}]\dot{\boldsymbol{\sigma}} - \mathbf{z}_2^T M S(1) M \boldsymbol{\delta} + k_s z_3) \quad (14)$$

where k_s is a positive constant, and the time derivative of V_3 becomes

$$\dot{V}_3 = -k_e \mathbf{e}_q^T M^{-1} \mathbf{e}_q - k_z \mathbf{z}_2^T \mathbf{z}_2 - k_s z_3^2 + \mathbf{e}_q^T \boldsymbol{\delta} - \mathbf{e}_q^T R^T \dot{\mathbf{q}}_d \quad (15)$$

It should be noted that the last two terms in (15) have uncertain signs. Before making further analysis, considering the practical operating conditions, we assume that $\dot{\mathbf{q}}_d$ is bounded. For notation simplicity, we define $\mathbf{e}_q = [e_1, e_2]^T$ and $R^T \dot{\mathbf{q}}_d = [\gamma_1, \gamma_2]^T$. Then, (15) can be expanded as

$$\begin{aligned} \dot{V}_3 = & -k_e \left(\frac{1}{m_{11}} e_1^2 + \frac{1}{m_{22}} e_2^2 \right) - k_z \mathbf{z}_2^T \mathbf{z}_2 - k_s z_3^2 + \\ & e_1 (\delta_1 - \gamma_1) + e_2 (\delta_2 - \gamma_2) \end{aligned} \quad (16)$$

We split the coefficient k_e into three parts: $k_e = k_1 + k_2 + k_3$, where $k_i > 0$ are positive scalar, and then rearrange (16) as

$$\begin{aligned} \dot{V}_3 = & -k_1 \mathbf{e}_q^T M^{-1} \mathbf{e}_q - k_z \mathbf{z}_2^T \mathbf{z}_2 - k_s z_3^2 - \\ & k_2 \left(\frac{e_1}{m_{11}} - \frac{m_{11}}{2k_2} \delta_1 \right)^2 - k_2 \left(\frac{e_2}{m_{22}} - \frac{m_{22}}{2k_2} \delta_2 \right)^2 + \frac{\|M\boldsymbol{\delta}\|^2}{4k_2} - \\ & k_3 \left(\frac{e_1}{m_{11}} + \frac{m_{11}}{2k_3} \gamma_1 \right)^2 - k_3 \left(\frac{e_2}{m_{22}} + \frac{m_{22}}{2k_3} \gamma_2 \right)^2 + \frac{\|M\boldsymbol{\gamma}\|^2}{4k_3} \end{aligned} \quad (17)$$

where $\|\cdot\|$ represents the Euclidean norm and $\boldsymbol{\gamma} = [\gamma_1, \gamma_2]^T$. Since M is a constant positive definite matrix and $\boldsymbol{\delta}$ is a given constant vector, the terms $M\boldsymbol{\delta}$ and $M\boldsymbol{\gamma}$ are always bounded, i.e., there exists a positive constant ζ such that $\|M\boldsymbol{\delta}\|^2/4k_2 + \|M\boldsymbol{\gamma}\|^2/4k_3 \leq \zeta$. Thus, (17) becomes

$$\dot{V}_3 \leq -k_1 \mathbf{e}_q^T M^{-1} \mathbf{e}_q - k_z \mathbf{z}_2^T \mathbf{z}_2 - k_s z_3^2 + \zeta \leq -\lambda V_3 + \zeta$$

where $\lambda = \min \left\{ \frac{2k_1}{m_{22}}, \frac{2k_z}{m_{22}^2}, \frac{2k_s}{m_{33}} \right\}$ because $m_{11} < m_{22}$ holds, and hence, by employing the Comparison Lemma^[11], we have

$$V_3(t) \leq V_3(0)e^{-\lambda t} + \frac{\zeta}{\lambda}, \quad t \geq 0 \quad (18)$$

which implies that V_3 globally converges to a bounded ball of radius ζ/λ around zero, and hence the states of error dynamics $(\mathbf{e}_q, \mathbf{z}_2, z_3)$ remain in a bounded set about the origin.

Remark 1. In reality, the physical actuators are subject to saturation because of their maximum and minimum limits, i.e., $F \in [F_{\min}, F_{\max}]$ and $s \in [s_{\min}, s_{\max}]$, which can affect the stabilization of the error dynamics. To depict this property, we define a saturation function as

$$\text{sat}(a) = \begin{cases} a_{\min}, & a < a_{\min} \\ a, & a \in [a_{\min}, a_{\max}] \\ a_{\max}, & a > a_{\max} \end{cases}$$

where a_{\min} and a_{\max} are the minimum and maximum value of a , respectively.

As mentioned above, a system may be just locally stable because of the saturation of control inputs. For simplicity, in this paper, we do not seek to design an optimal control law for system (5) to reduce the undesired effects of the inputs constraints, but first estimate a region of initial states errors which can be forced to around zero by approximately calculating (11) and (14) with given inputs bounds and control gains.

3 Point mass positioning control

Actually, the displacement s , which determined by the force w_1 from (4), is not a real control input. To accomplish the control development, we design a servo control law for w_1 in this section. Since the term s in (14) is actually the commanded displacement of the point mass, for the sake of clarity, we use a new character s_c to replace it.

Before s_c is invariant in each step of the control course, i.e., its first time derivative or more is zero. This is because the point mass would prefer to keep rest if its commanded displacement is completed in one time step.

Let $z_s = s - s_c$ be the point mass positioning error. Then using (4), we obtain

$$\dot{z}_s = \dot{s}, \quad \ddot{z}_s = \ddot{s} = s r^2 - \frac{1}{m} w_1 \quad (19)$$

To make the error z_s converge to zero, we introduce a virtual control law for w_1

$$w_1^d = m(k_d \dot{s} + s r^2 + k_p z_s) \quad (20)$$

in which k_d and k_p are positive constant gains. Then, the dynamics of z_s is given by

$$\ddot{z}_s + k_d \dot{z}_s + k_p z_s = 0$$

which implies that z_s converges to zero. However, in reality, the executive devices that actuated on the moving mass

always respond sluggishly. To depict this character, we model the devices dynamics as

$$T\dot{w}_1 + w_1 = w_{1c} \quad (21)$$

where T is a positive constant, and w_{1c} represents the commanded input. Let $w_{1e} = w_1 - w_1^d$ be the control error. Then we get

$$\dot{w}_{1e} = \frac{1}{T}(w_{1c} - w_1) - \dot{w}_1^d \quad (22)$$

We set w_{1c} at $w_{1c} = w_1 + T\dot{w}_1^d - k_w T w_{1e}$, where k_w is a positive scalar, and thus, (22) can be rewritten as

$$\dot{w}_{1e} = -k_w w_{1e} \quad (23)$$

From (19)~(23), we can express the dynamics of the point mass subsystem in a cascaded form

$$\begin{cases} \dot{z}_s \\ \ddot{z}_s \\ \dot{w}_{1e} \end{cases} = \begin{bmatrix} 0 & 1 \\ -k_p & -k_d \end{bmatrix} \begin{bmatrix} z_s \\ \dot{z}_s \end{bmatrix} + \begin{bmatrix} 0 \\ 1 \end{bmatrix} w_{1e} \quad (24)$$

As discussed in [12], subsystem (24) is globally asymptotically stable, which implies that $\lim_{t \rightarrow \infty} z_s = 0$.

Remark 2. We separate the control designing course of w_1 from that of the AUV tracking problem because this operation can reduce the complexity of the whole design procedure without affecting the stability of the resulting closed-loop system. Since the length of the slot l is short because of the limitation of the hull, implying that z_s and its time derivatives are small, we can assume that the saturation of w_1 will not occur in practice.

Remark 3. At each time step in our numerical computation, we set the term s and its time derivative \dot{s} in w_2 and w_3 at the value at the previous step. This operation facilitates the designing course because w_2 and w_3 are already known now. The additional errors in the model aroused by this simplification are tolerable and would not affect the main results we have received.

4 Numerical results

To illustrate the performance of the proposed method, we present some numerical results in this section. The parameters of the AUV are given as^[10,13]: $m_{11} = 215$ kg, $m_{22} = 265$ kg, $m_{33} = 80$ kg \cdot m², $X_u = 70$ kg/s, $X_{u|u|} = 100$ kg/m, $Y_v = 100$ kg/s, $Y_{v|v|} = 200$ kg/m, $N_r = 50$ kg \cdot m²/s, $N_{r|r|} = 100$ kg \cdot m². Moreover, the control inputs are limited at $F \in [0, 500]$ N and $l = 0.2$ m. The point mass $m = 1.0$ kg. The simulation is implemented on Simulink by using a fixed-step fourth order Runge-Kutta method whose step size is 0.1 s.

The parameters of the desired trajectory to be tracked are given as: $x_d = 0.01t + 0.1$ and

$$y_d = \begin{cases} -0.2, & 0 \leq t \leq 300 \\ 2 \cos(0.01t) - 2.2, & 300 < t \leq 300 + 100\pi \\ -4.2, & t > 300 + 100\pi \end{cases}$$

It is worth noting that the rest parameters of the desired trajectory are not required to be known because of the proposed controller. For the AUV, we choose the initial conditions as $(x(0), y(0), \theta(0), u(0), v(0), r(0)) = (0, 0, 0, 0, 0, 0)$ which implies that the AUV starts from rest and the initial position errors are $x_e(0) = -0.1$ m and $y_e(0) = 0.2$ m. The set error vector $\delta = [-0.01, 0]^T$ and the control parameters are chosen as follows: $k_e = k_z = k_s = 30$, $k_d = 1$, $k_p = 0.8$,

and $k_w = 10$. We first consider the case where the disturbances $\tau_{di} = 0$, $1 \leq i \leq 3$. The numerical results are shown in Figs. 2~4. It can be seen that the tracking errors converge and stay at a small neighborhood of zero.

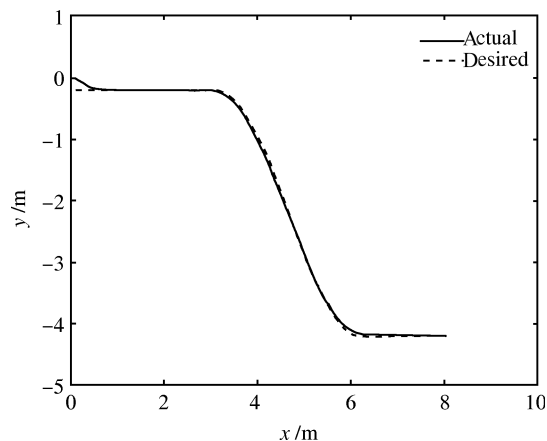


Fig. 2 The trajectories of the AUV

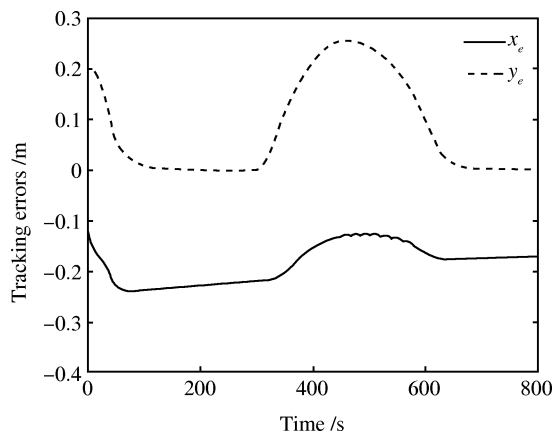


Fig. 3 The tracking errors

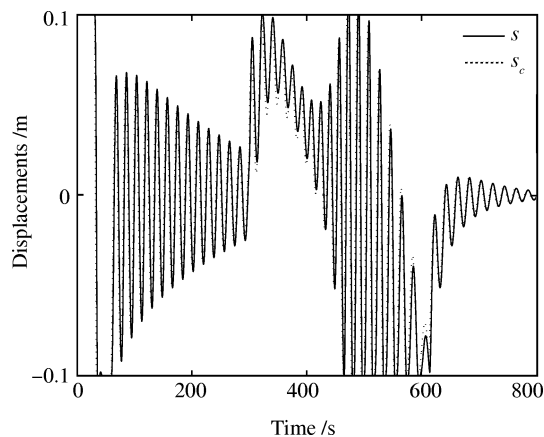


Fig. 4 The displacements of the point mass

To illustrate the robustness properties of the designed trajectory-tracking methodology, we present some results under external disturbances and model uncertainties, i.e., the disturbances $\tau_{di} \neq 0$, $1 \leq i \leq 3$. We assume that there are inaccuracies of the order of 5% in the AUV model. The

initial conditions and the desired trajectory are the same as those of the previous example. The control parameters are chosen as follows: $k_e = k_z = k_s = 100$, $k_d = 1$, $k_p = 0.8$, and $k_w = 15$. The results are shown in Figs. 5~7. One can see that the errors still within a small neighborhood of the origin.

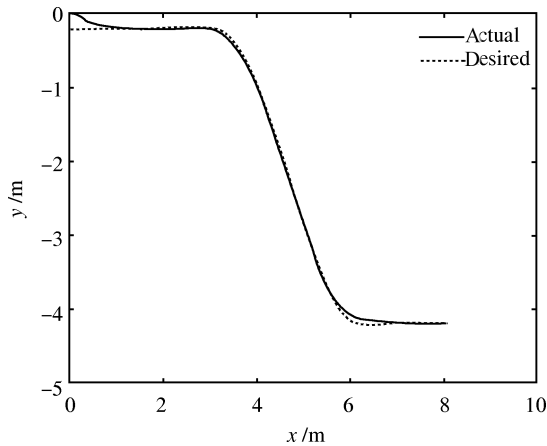


Fig. 5 The trajectories of the AUV

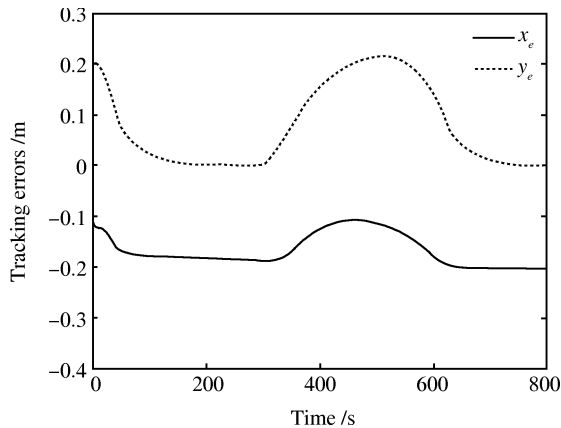


Fig. 6 The tracking errors

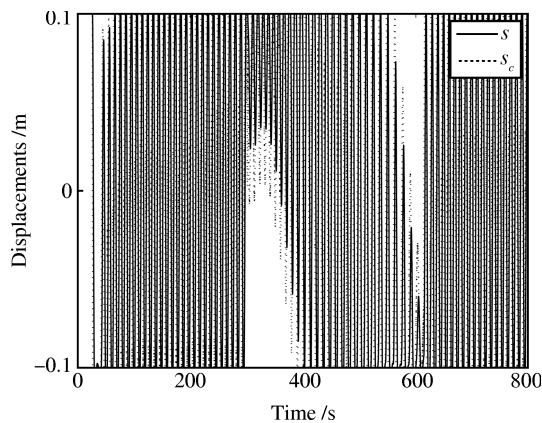


Fig. 7 The displacements of the point mass

Note that the desired velocity of the AUV in these examples is $\sqrt{\dot{x}_d^2 + \dot{y}_d^2} < 0.025$ m/s. Moreover, the maximum magnitude of torque in yaw is required to be more than

1.0 N·m, and hence the conventional actuators such as fins and rudders will lose their effectiveness in this case.

5 Conclusion

In this paper, the problem of trajectory-tracking was investigated for an AUV moving in the vertical plane with the aid of an internal moving mass. Combined with the dynamics of the point mass, the AUV was modeled as an underactuated system. A Lyapunov-based tracking control law was proposed by using backstepping approach to guarantee the tracking errors to converge and remain in a small neighborhood about zero. The numerical results showed that the proposed method has good tracking performance and a certain robustness against modeling errors.

References

- 1 Woolsey C A, Leonard N E. Stabilizing underwater vehicle motion using internal rotors. *Automatica*, 2002, **38**(12): 2053–2062
- 2 Menon P K, Sweriduk G D, Ohlmeyer E J, Malyevac D S. Integrated guidance and control of moving mass actuated kinetic warheads. *Journal of Guidance, Control, and Dynamics*, 2004, **27**(1): 118–126
- 3 Wang S Y, Yang M, Wang Z C. Moving-mass trim control system design for spinning vehicles. In: Proceedings of the 6th World Congress on Intelligent Control and Automation. Harbin, China: IEEE, 2006. 1034–1038
- 4 Petsopoulos T, Regan F J, Barlow J. Moving-mass roll control system for fixed-trim re-entry vehicle. *Journal of Spacecraft and Rockets*, 1996, **33**(1): 54–60
- 5 Woolsey C A, Leonard N E. Moving mass control for underwater vehicles. In: Proceedings of the American Control Conference. Anchorage, USA: IEEE, 2002. 2824–2829
- 6 Leonard N E, Graver J G. Model-based feedback control of autonomous underwater gliders. *IEEE Journal of Oceanic Engineering*, 2001, **26**(4): 633–645
- 7 Aguiar A P, Hespanha J P. Trajectory-tracking and path-following of underactuated autonomous vehicles with parametric modeling uncertainty. *IEEE Transactions on Automatic Control*, 2007, **52**(8): 1362–1379
- 8 Jiang Z P. Global tracking control of underactuated ships by Lyapunov's direct method. *Automatica*, 2002, **38**(2): 301–309
- 9 Repoulas F, Papadopoulos E. Planar trajectory planning and tracking control design for underactuated AUVs. *Ocean Engineering*, 2007, **34**(11-12): 1650–1667
- 10 Fossen T I. *Guidance and Control of Oceanic Vehicles*. New York: Wiley, 1994
- 11 Khalil H K. *Nonlinear Systems (Second Edition)*. New York: Prentice Hall, 1996
- 12 Lefeber E, Pettersen K Y, Nijmeijer H. Tracking control of an underactuated ship. *IEEE Transactions on Control Systems Technology*, 2003, **11**(1): 52–61
- 13 Fjellstad O E, Fossen T I. Position and attitude tracking of AUV's: a quaternion feedback approach. *IEEE Journal of Oceanic Engineering*, 1994, **19**(4): 512–518

LI Jia-Wang Ph.D. candidate at College of Marine, Northwestern Polytechnical University. His research interest covers modeling and control of marine systems with applications to separable AUVs. Corresponding author of this paper. E-mail: ljw1024@mail.nwpu.edu.cn

SONG Bao-Wei Received his Ph. D. degree from Northwestern Polytechnical University in 1999. He is currently a professor at College of Marine, Northwestern Polytechnical University. His research interest covers system reliability designing and optimization of marine vehicles. E-mail: songbaowei@nwpu.edu.cn

SHAO Cheng Ph. D. candidate at College of Marine, Northwestern Polytechnical University. His research interest covers modeling and control of underwater towed cable systems. E-mail: yaoyaochi@163.com